EVALUATION OF DISLOCATION STRUCTURE AND CRYSTALLITE SIZE IN WORN AL-SI ALLOY BY X-RAY DIFFRACTION

A. Rezvanifar and M. Zandrahimi
m.zandrahimi@mail.uk.ac.ir
Received: August 2009 **Accepted: January 2010**

Department of Materials Science and Engineering, Shahid Bahonar University of Kerman, Kerman, Iran.

Abstract: *Diffraction peak profile analysis has recently been developed to such an extent that it can be applied as a powerful method for the characterization of microstructures of crystalline materials in terms of crystallite size and dislocation structures. In this paper the effect of the sliding on the microstructure of A356 in the as-cast and heat treated conditions are studied, The X-ray phase analysis shows that with increasing applied load, the dislocation density is increased, whereas the crystallite size is decreased. It was found that heat treatment raised dislocation density during wear. The screw or edge character of dislocations in worn specimens were determined by analyzing the dislocation contrast factors, it was demonstrated that the character of the prevailing dislocations in high loads is nearly pure screw.*

Keywords: *Severe Wear, Peak Profile Analysis, Crystallite Size, Dislocation Structure*

1. INTRODUCTION

Strains, caused by shearing in sliding, are present some depth below the surface reaching the extreme values at the surface, that lead to break down the original grain structure at the Surface to form dislocation cells. These cells can be described as subgrain regions, which are separated by regions (walls) of highly tangled dislocations [1, 2]. A cellular structure directly beneath worn surfaces of metallic materials has been observed in transmission electron microscopy studies, Materials vary greatly in their tendency to form dislocation cells which, according to general metallurgical theory, depends on stacking fault energy, and i.e., high stacking fault energy promotes cell formation [3]. X-ray diffraction (XRD) is an effective tool for the determination of crystallite size distribution. X-ray diffraction line profiles are broadened due to the smallness of crystallites and the lattice distortions. The two effects can be separated on the basis of the different diffraction order dependence of peak broadening. The standard methods of x-ray diffraction profile analysis based on the full widths at half maximum (FWHM), the integral breadths, and the Fourier coefficients of the profiles provide the apparent crystallite size and the mean square strain [4-6]. The evaluation of x-ray profiles is further complicated by anisotropic strain broadening of the diffraction lines. This means that neither the full width at half maximum nor the integral breadth nor the Fourier coefficients of the profiles are monotonous functions of the diffraction vector [6,7] The strain anisotropy has been shown to be well accounted for by the dislocation model of the mean square strain by introducing the contrast factors of dislocations. Whereas the values of the dislocation contrast factors depend on the type of dislocations present in the crystal [8, 9] In this paper, the effect of dry sliding on the X-ray line broadening is studied and the microstructural parameters are characterized by X-ray diffraction profile analysis with using Williamson–Hall model, and correlation between sliding, dislocation density and crystalline size are investigated.

2. EXPERIMENTAL PROCEDURE

2.1. Sample Preparation and Experimental Techniques

An Al-Si alloy (A356) with chemical composition 6.6Si, 0.32 Mg, 0.25 Fe, 0.01 Cu, 0.004 Mn and Al balance (all values in wt%) were prepared by melting of purity Al (99.7%), Al-75%si, Al-50%Mg master alloy, master alloy were produced by mechanical alloying, in this process, the pure Al alloy was initially placed inside in a graphite crucible and they heated to 775°C in a resistance-heated furnace, pouring

[Downloaded from csc.iust.ac.ir on 2026-06-13]

temperature was controlled at about 725°C. Some of the cast alloys specimens were subjected to the T6 heat treatment (solution treated at 480°C for 4hr and aging at 180°C for 1hr). The alloys were polished, etched by a Keller solution and were observed by a Scanning Electron Microscopy (SEM). Tribological test were carried out by pin on disk machine under dry sliding condition at room temperature. disk of tested materials have (70mm*70mm*6mm) as wear samples, cylindrical pins of 5mm diameter and 50mm length with curvature radius 2mm made of high carbon chromium steel to a hardness of 59 HRC. test were carried out at constant sliding speed 0.21m/s. constant sliding distance 1000m and normal loads 50,100 and 150N both in the as-cast and T6 conditions.

The X-ray diffraction (XRD) profile for each sample was recorded from the worn surface by PHILIPS 1710 X-ray diffractmeter using the Cu Kα radiation. All the diffraction profiles were obtained by varying 2θ from 35 to 142° with a step scan of 0.02°, the time spent for collecting the data per step was 4s. The diffraction profiles were corrected for the instrumental broadening using a silicon sample, which had large crystallites and was free from defect broadening by Stokes method [10].

2.2. Theoretical Formulation

The classical Williamson-Hall plot can be solved for dislocated crystals and has been called the modified Williamson-Hall plot [8] is based on the *FWHM* and integral breadths for a profile; this plot is given as a function of $Kc^{1/2}$ instead of K in classical Williamson-Hall approach.

$$\Delta K_{FWHM} \cong 0.9/D + (\pi M^2 b^2/2)^{1/2}\rho^{1/2}(KC^{1/2})^2 + O(K^2C)^2 \quad (1)$$

Where $\Delta K_{FWHM} = (\cos(\theta/\lambda)\Delta 2\theta$, θ is the Bragg angle and $\Delta(2\theta)$ is the *FWHM* or the integral breadth, D is an apparent crystallite size $K = 2\sin\theta/\lambda$, M is a constant depending on the dislocations and ρ are the Burgers vector and the average density of dislocations, respectively, and *O* stands for higher-order terms in $KC^{1/2}$ and *C* is average contrast factors of dislocations becomes a simple fourth order function of the indices of different reflections in cubic systems. The contrast factors are averaged over the permutation of indices and is given as:

$$\overline{C} = A - B(h^2k^2 + k^2l^2 + l^2h^2)/(h^2 + k^2 + l^2)^2 \quad (2)$$

Where A and B are constants and depends upon the elastic constants of the materials. The value of A is the average contrast factor corresponding to the indices $\overline{C}_{h00}$, i.e $\overline{C}_{h00} = A$ Also the average indices in Eq. (2) is denoted as q = B/A and becomes,

$$\overline{C} = \overline{C}_{h00}(1 - qH^2) \quad (3)$$

Where,

$$H^2 = (h^2k^2 + k^2l^2 + l^2h^2)/(h^2 + k^2 + l^2)^2$$

This equation shows that for untextured polycrystals or randomly populated slip system, average contrast factors can be evaluated if the values of 'q' and '$\overline{C}_{h00}$' are known for that material. Depending on the value of 'q' factor the type of dislocation may be screw type or edge type or half crew-half edge type [11, 12]. Ungar et all [8] suggested methods for calculating both the theoretical and experimental 'q' factors and also the $\overline{C}_{h00}$ using simple analytical function. Combining Eqs. (1) And (3) the following equation can be obtained which is used for determination of 'q' factor.

$$\left[(\Delta K)^2 - \alpha\right]K^2 \cong \beta\overline{C}_{h00}(1 - qH^2) \quad (4)$$

3. RESULTS AND DISCUSSIONS

3.1. X-ray Analysis

Fig.1 shows a typical X-ray diffractrogram of alloy before and after wear in the as-cast and heat treated condition. As it is clearly shown, all the possible α-Al and Si phase reflections are expectedly present. As shown in Fig.1 b and d, after wear, the normalized intensity of the peaks decreases which could be due to increase in the density of vacancies [13]. This is negligible for T6 heat treated specimens. The relative intensities of the Si reflection are much higher

[Downloaded from csc.iust.ac.ir on 2026-06-13]

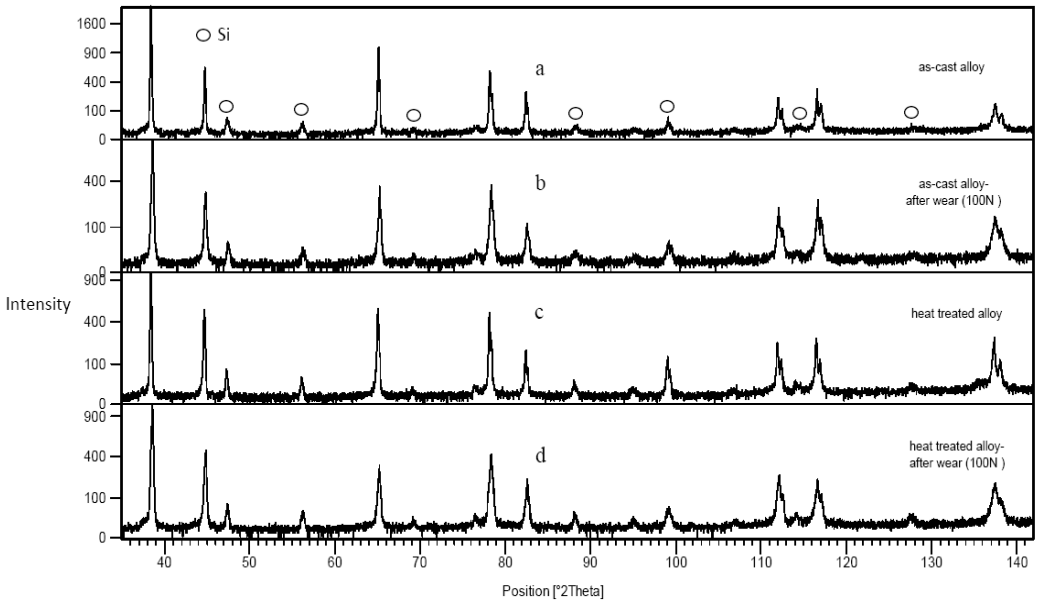

Fig. 1. X-ray diffraction patterns of the alloy: (a) before wear (b) after wear (100N) (c) heat treated alloy (d) heat treated alloy after wear (100N).

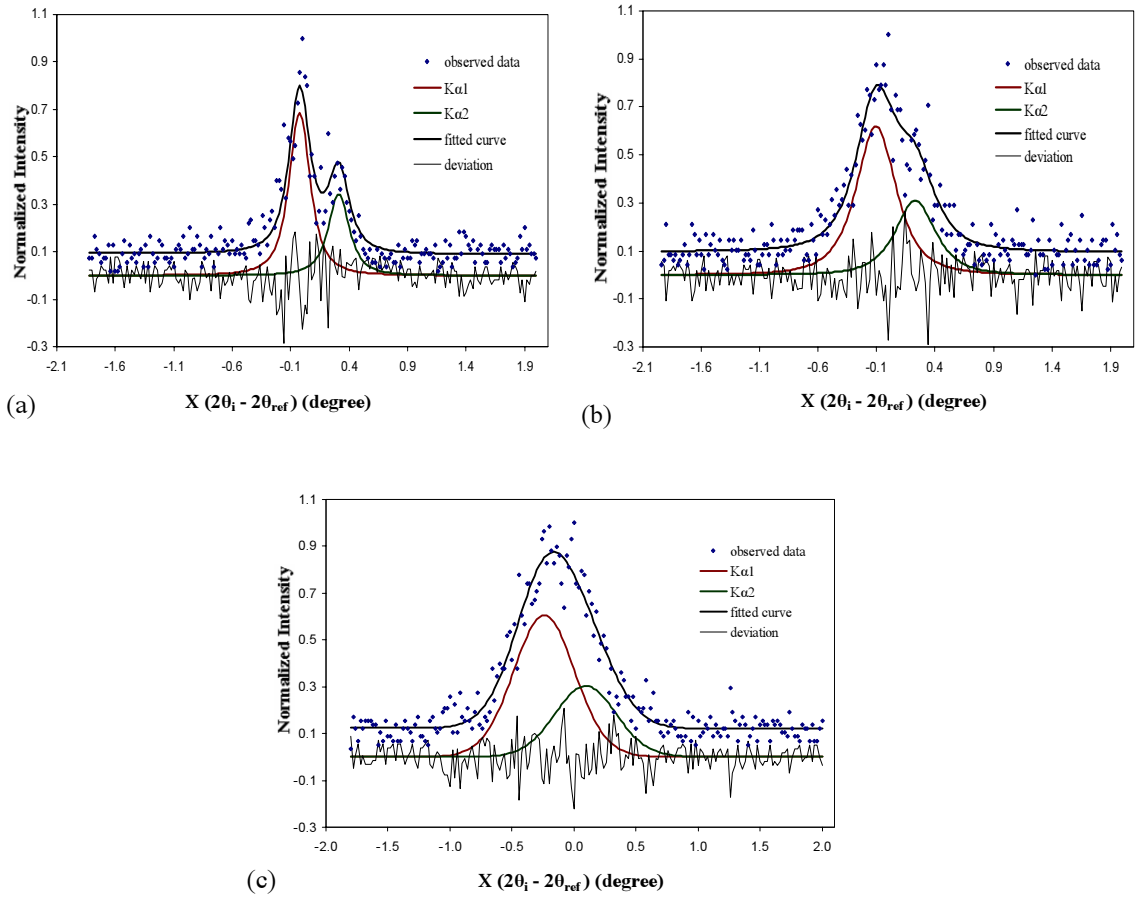

Fig. 2. The measured and the fitted curve via Pearson function corresponding to the 400 reflections of Al: (a). before wear (b). 100N (c). 150N, the difference between the measured and the fitted values is also plotted in the lower parts.

[Downloaded from csc.iust.ac.ir on 2026-06-13]

after heat treatment as shown in Fig.1, indicating that heat treatment results in separation of Silicon from the matrix. Moreover, after heat treatment, the peaks shift to higher angles which is the indication of reduction in lattice parameter (Note: for the as cast and heat treated samples, peak shift is only related to the Si concentration in the solid solution). The increase in aluminum lattice parameter is as a result of decrease in Si concentration in it which is caused by the difference between atomic radii of aluminum and silicon (r_{Al} = 0.1428 nm and r_{Si} = 0.117 nm).

Utilizing the PearsonVII function, the broadening, due to strain and crystallite size, is obtained and shown in Fig 2. a-c). This gives reasonable approximation when the line profile is adjusted to a combination of Lorentzian and Gaussian functions. It illustrates comparison between experimental measured intensity and fitted curve of (400) diffraction peaks. A continuous broadening of the diffraction peaks, due to disintegration and plastic deformation of particles, is evident with increasing applied load which excesses the amount of overlapping. Difference between the measured and the fitted values is also plotted in the lower parts of the figures with the same scaling as in the main parts of the figures.

3.2. Microstructural Characterization

SEM microphotographs of the cast and heat-treated alloys are shown in Figs. 3a-d. As shown, the microstructure of as cast (Fig. 3a) consists of the eutectic mixture of α-aluminum and silicon along the grain boundaries of primary α-aluminum grains. During heat treatment, dendritic structure is broken down, besides, spheroidization and enhanced distribution of Si,

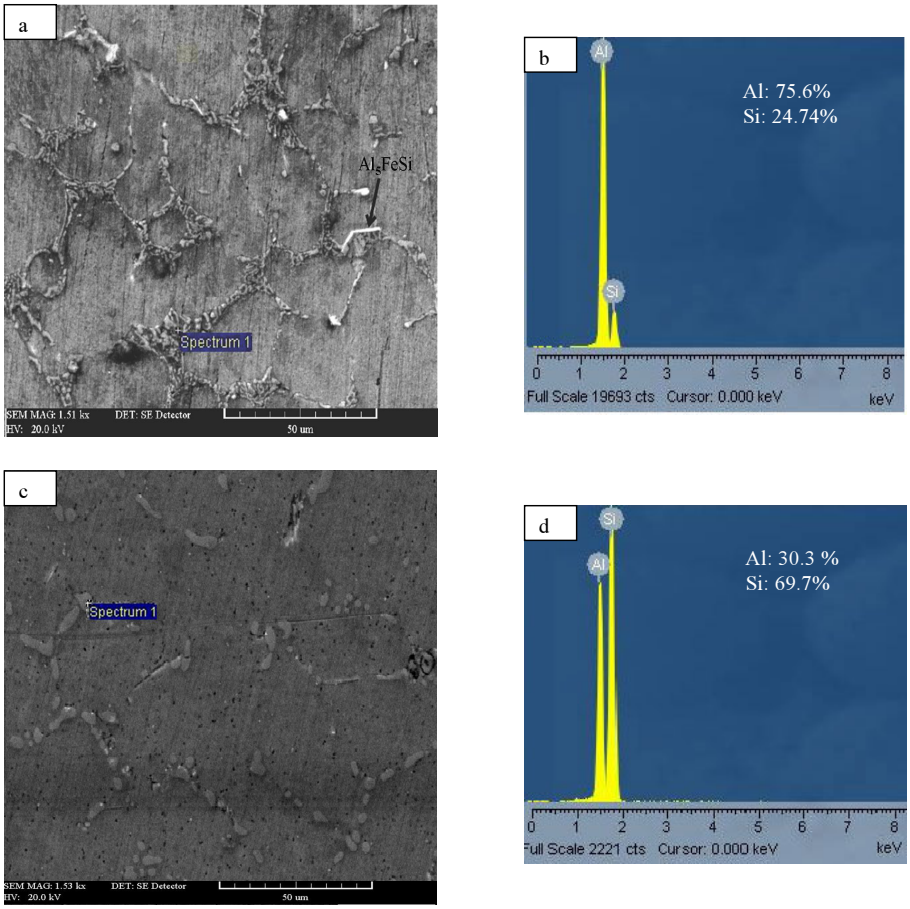

Fig. 3. (a) and (c): SEM secondary electron images of the alloy as-cast and T6 treated; (b) and (d): EDS spectrum of the eutectic compounds of the alloy as-cast and T6 treated

[Downloaded from csc.iust.ac.ir on 2026-06-13]

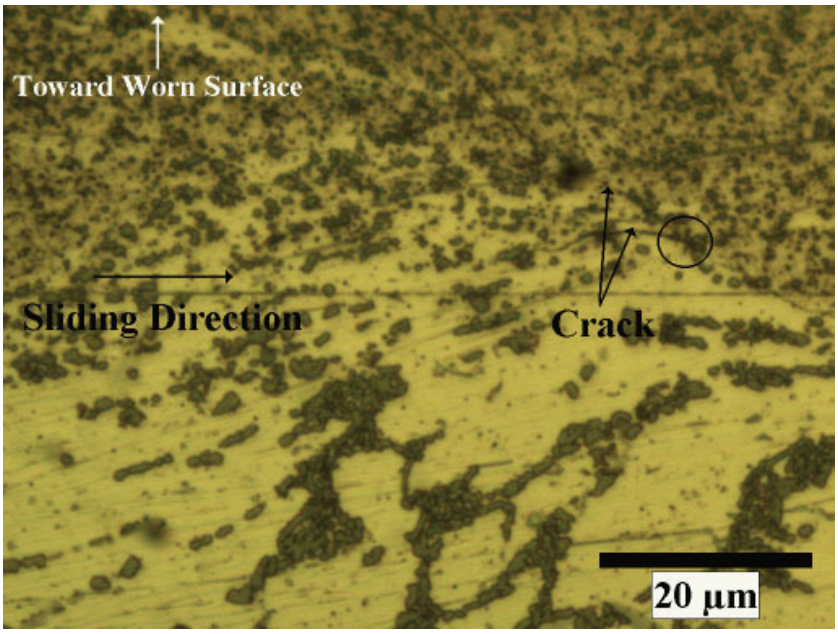

Fig. 4. Optical Micrograph of subsurface of worn specimen at 100N showing plastic deformation in the direction of sliding. The arrows indicate the cracks in the subsurface, and the circle suggests Al-Si eutectic led to crack deflection.

as well as refinement of eutectic silicon particles take place. As a result of heat treatment, cast structure is modified; furthermore, Si concentration in eutectic is increased (Fig. 3b,d) which is confirmed by XRD results.

Fig. 4 presents the optical micrograph of typical cross-section of the wear subsurface. As it can be seen, the microstructural features of the subsurface vary along the depth below the worn surface. The eutectic Si colonies are elongated in the direction of sliding, suggesting plastic deformation and a shear strain gradient in the subsurface which are generated during the sliding wear. A prominent feature is the morphology of the top surface layer which containes very fine particles and agglomerates. The cracks, originating at various points, propagates parallel to the surface of disk and nucleate at one point which result in the removal of debris.

3.3. Determination of 'q' factor

The value of the quantity 'q', as defined in Eq. (3), differentiates the type of dislocation. To

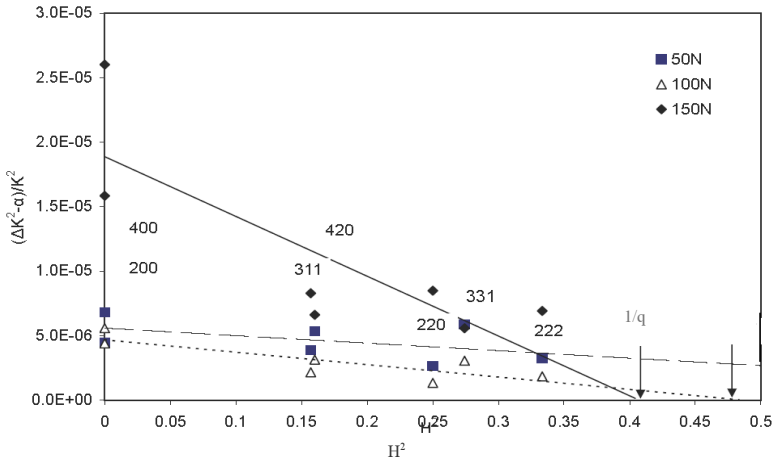

Fig. 5. The FWHM of worn surfaces plotted for determination of 'q' factor according to equation (4).

[Downloaded from csc.iust.ac.ir on 2026-06-13]

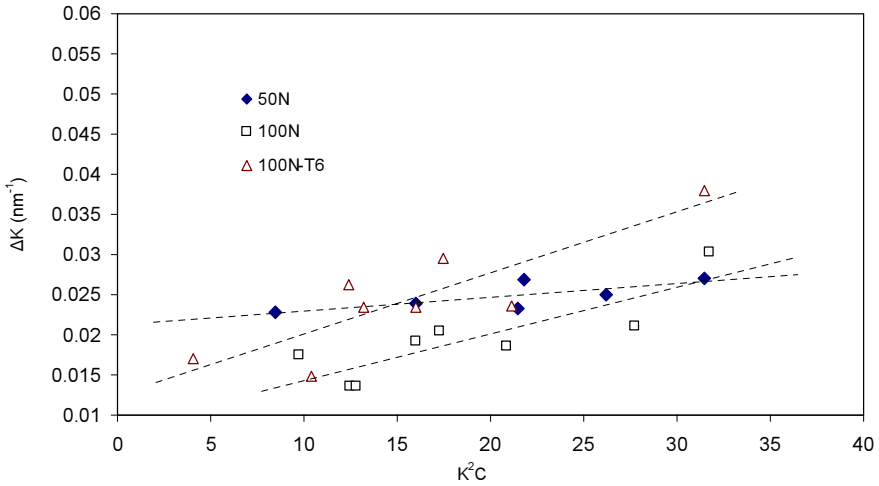

Fig. 6. Modified Williamson–Hall plot from expression (1) in the text.

Table 1. q Parameter value outcome of Fig.4

Load / N	Before wear	50	100	150	T6	T6-100
q	0.37	0.97	2.07	2.44	0.65	2.017

evaluate the factor 'q', a quantity $\left[(\Delta K)^2 - \alpha\right] K^2$ versus H^2 is plotted according to Eq. (4), then a straight line is fitted (Fig. 5). The intercept of H^2 axis gives the value of 1/q. The *q* parameter values for aluminum, corresponding to pure screw and edge dislocations in the <1 10> {1 1 1} slip systems, are determined by detailed numerical calculations using elastic constants from [8]. This yielded the *q* values of 1.36 or 0.33 for pure screw or edge dislocations, respectively. As shown in table.1, the experimental value of *q* is found to be 0.37 in cast alloy which is very near to the theoretical value of 0.33 corresponding to edge dislocation. This indicates that the dislocations have more edge character than screw character. For the worn surface at applied load of 50 N, the value of *q* is found to be 0.9750 which is equivalent to the approximate arithmetic average of the two numerically calculated *q* values. The straightforward interpretation of this result is that the character of the prevailing dislocations is half edge, half screw. A definite tendency of the increase of the *q* parameter with the applied load can be observed, indicating that the screw character becomes stronger with increasing deformation. For the applied load of 150N, the experimental value, q_{exp} = 2.44, is out of mentioned range. The discrepancy can be solved by finding a type of dislocation which is still compatible with the f.c.c. lattice but provides a larger range for the values of *q*, which prove the occurrence of severe wear.

3.4. Evaluation of Submicron Grain Size and Dislocation Density

As it is assumed that the peak widths at intensities above shoulders are related to strain broadening caused by dislocations and to fine particles size broadening caused by small coherent domain size of the deformed materials. It is necessary to plot 'MWH' to subtract the particle-size broadening by taking into account strain anisotropy [14]. The ΔK_{FWHM} versus K^2C is shown in Fig. 6. For the first eight Bragg reflections, according to modified Williamson-Hall (W-H) plot, the FWHM increases with K^2C in a global scale indicating the presence of lattice distortion. As it is shown in Table 2, the intersection at K = 0 gives the average particle size corresponding to the FWHM and the plot slope is proportional to $\sqrt{\rho}$. It is clearly evident from table 2 a considerable decrease of crystallites size and enhancement in dislocation density can be

[Downloaded from csc.iust.ac.ir on 2026-06-13]

Table 2. Mean Crystallite size and linear slope as a result of mWH plot (ñ: dislocation density)

Load / N	Before wear	50	100	150	T6	T6-100
Particle size	58.47μm	42.96nm	87.419nm	34.867nm	1937.727nm	71.825nm
Slope α $\rho^{1/2}$	0.000384	0.000177	0.000505	0.000899	0.000285	0.00076

obtained after wear which persists up to applied load of 150N. The amount of broadening for the applied load of 50N sample is more than 100N (Fig. 6), whereas dislocation density is vice versa (Table 2). Thus broadening in 50N is mainly due to the apparent size induced anisotropic strain broadening. At low loads during wear high resistance of MML (mechanical mixed layer) are responsible for the production of too many subgrains in the subsurface. As the result of heat treatment spheroidization of eutectic phase and distribution of fine precipitates in the matrix take place which act as obstacles on dislocation motion, and, consequently, lead to increase in hardness and strength. In addition this causes fewer tendencies which eventually raises the dislocation density (Table 2).

4. CONCLUSIONS

1. X-ray analysis showed important broadening of the diffraction lines after wear; furthermore, the relative intensity of the diffraction peaks was strongly decreased.
2. Quantitative data obtained from the Williamson-Hall plot indicated that the average particle size attained for 150N load was 35nm. An increase of the dislocation density was observed with enhancement in the applied load.
3. The dislocation factor q was calculated and it was found that for high loads the type of dislocation is predominantly screw.

REFERENCES

1. Rigney, D. A. and Glaeser, W. A., *The Significance of Near Surface Microstructure in the Wear Process. Wear*., 1978, 46, 241-250.
2. Garbar, I. I. and Skorinin, J. V., *Metal Surface Layer Structure Formation under Sliding Friction*. *Wear*., 1978, 51, 327-336.
3. Stachowiak, W., Engineering tribology, 3rd Ed, 2005, pp. 560-650.
4. Gubicza, J., Ribarik, G., Bakonyi, I. and Ungar, T, Crystallite-Size Distribution and Dislocation Structure in Nanocrystalline HfNi5 Determined by X-Ray Diffraction Profile Analysis. Nanoscience and Nanotechnology., 2001, 1, 1-6.
5. Warren, B. E., Prog .Metal phys, 1959, 8, 147.
6. Gubicza, J., Kassemc, M., Ribarik, G. and Ungar, T., *The microstructure of mechanically alloyed Al–Mg determined by X-ray diffraction peak profile analysis. Materials Science and Engineering A*., 2004, 372, 115–122.
7. Scardi, P. and Leoni., M. J. Appl. Cryst., 1999, 32, 671.
8. Ungar, T. and Brobely, A. Appl. Phys. Lett., 1996, 69, 3173.
9. Wilken, M., *The Determination of Density and Distribution of Dislocations in Deformed Single Crystals from Broadened X-Ray Diffraction Profiles. Phys. Status solid A.*, 1970, 2, 359.
10. Stokes, A. R., *A Numerical Fourier-analysis Method for the Correction of Widths and Shapes of Lines on X-ray Powder Photographs. Appl. Phys.*, 1948, 382-390.
11. Zehetbauer, M. J. and Zhu, Y. T. Bulk Nanostructured Materials., 2009, 361-380.
12. Dey, S. N., Chatterjee, P. and Sen Gupta, S. P., *Dislocation induced line-broadening in cold-worked Pb-Bi binary alloy system in the a-phase using X-ray powder profile analysis. Acta Materialia.*, 2003, 51, 4669–4677.
13. Guinebretière, R., X-ray Diffraction by Polycrystalline Materials. 1Ed, USA, 2007, pp. 200–210.
14. Eskin, D. G., Massardier, V. and Merle, P. J. Mater. Sci., 1999, 34, 811–820.

[Downloaded from csc.iust.ac.ir on 2026-06-13]